

Spectral Color Reproduction using an Interim Connection Space-Based Lookup Table

Shohei Tsutsumi*, Mitchell R. Rosen† and Roy S. Berns‡

*Canon Inc.; Tokyo, Japan;

†Munsell Color Science Laboratory, Rochester Institute of Technology; Rochester, New York, USA

Abstract

For purposes of defining a feasible approach to spectral color management, previous research proposed an interim connection space (ICS). ICS is relatively low in dimensions and would be situated between a high-dimensional spectral profile connection space and output units. The current research simulated printed spectra after using a multi-dimensional ICS-based lookup tables (LUTs) based on LabPQR, an ICS described in earlier work. LabPQR has three colorimetric dimensions (CIELAB) and additional dimensions to describe a metameric black (PQR). The spectral reproduction accuracies for printing on a six-color ink-jet printer were compared based on several versions of the ICS-based LUTs. Variations were evaluated with respect to quality trade-offs between size of the LUT and spectral reproduction accuracies, as well as the number of dimensions necessary for spectral color management. A five-dimensional 17x17x17x5x3 LUT performed well with three dimensions for CIELAB and two dimensions for the PQR metameric black space. This LUT resulted in average CIEDE2000 of 0.51 and average spectral RMS error of 4.22 % for a simulated spectral reproduction of the GretagMacbeth Color Checker.

Introduction

An important goal of spectral color management is to reproduce images that match originals under arbitrary illuminants. Spectral reproduction requires new approaches including spectral profiling of devices, spectral profile connection spaces (PCS λ), spectral-image processing and new quality metrics. Spectral color management will take advantage of all these concepts and require transformation chains that deliver high-quality results quickly.

In previous research [1]-[3], a spectral reproduction workflow from scene to hardcopy was proposed. One of the difficulties associated with spectral reproduction is its high dimensionality since more information is necessary for reproducing samples with illuminant-independence than needed for more traditional colorimetric reproduction. The proposed workflow included a step where spectra of high dimensionality were converted to a lower-dimensional encoding known as an interim connection space (ICS) [3]-[4].

Derhak and Rosen proposed an ICS called LabPQR [5]-[6]. LabPQR is an ICS that has three colorimetric axes (CIELAB) plus additional spectral reconstruction axes (PQR). PQR describes a stimulus' metameric black [7]-[8], a spectral difference between the actual spectra and a spectra derived from only knowledge of the CIELAB components. In a transformation to spectra from the LabPQR encoding, one of the infinite possible spectra is derived from CIELAB values and is combined with a metameric black correction derived from the PQR encoding. One approach

described in the literature for building LabPQR [5] uses the spectral gamut of a particular output device to derive the transformation from CIELAB to a metamer.

Tsutsumi, Rosen, and Berns have explored the influence of dimensional reduction in the metameric black axes of LabPQR [9]. It was found that a five-dimensional LabPQR (only two metameric black dimensions) achieved equivalent levels of performance to a full 31-dimensional approach when the limited spectral gamut of a printer was taken into account. For use in a real system, it may well be necessary to build a multi-dimensional lookup-table (LUT) to convert from ICS to device digits.

Hung [10] has examined linear and non-linear interpolation techniques for several different sizes of three-dimensional LUTs, and discussed interactions between the interpolation techniques and LUT size with respect to colorimetric matching. Balasubramanian [11] has explored cost reduction of LUT based on color transformation, in addition to the consideration of LUT size.

This research analyzes a simulation of spectral color reproduction using an ICS-based LUT. The ICS chosen here was LabPQR. Spectral reproduction accuracies for different versions of the ICS-based LUT are illustrated and compared to a traditional three-dimensional colorimetric-based LUT and a direct inversion method for spectral reconstruction. Quality trade-offs between memory size and spectral reproduction accuracies are discussed in terms of both colorimetric and spectral matching.

Theory

LabPQR

LabPQR [5]-[6] is an interim connection space (ICS) for use in spectral color management. The first three dimensions are CIELAB values under a particular viewing condition, and the additional dimensions are used for spectral reconstruction (PQR). A six-dimensional example of LabPQR has been discussed in the literature [5]-[6] and it has been demonstrated for use in spectral gamut mapping [6],[9],[12].

Spectral reconstruction from the LabPQR spaces as used herein follows the algorithm below:

$$\hat{\mathbf{R}} = \mathbf{T}\mathbf{N}_c + \mathbf{V}\mathbf{N}_p, \quad (1)$$

where \mathbf{T} is a n by 3 transformation matrix with n samples along wavelength, \mathbf{V} is a n by 3 matrix describing PQR bases, \mathbf{N}_c is a 3 by 1 tristimulus vector, and \mathbf{N}_p is a 3 by 1 vector of PQR values. Here, the subscripts "c" and "p" denote colorimetric and PQR values, respectively. Note that \mathbf{T} is applied to tristimulus values converted from CIELAB coordinates.

The derivation of the \mathbf{V} matrix depends on both the nature of the metamer created through the \mathbf{T} matrix from LabPQR's

CIELAB dimensions and the spectral gamut that is being described by the ICS. An approach that does not impose *a priori* constraints on derivation of the \mathbf{T} matrix is derived directly from the spectral space of the device being profiled. The \mathbf{T} matrix is determined by a matrix calculation using least square analysis with the use of the tristimulus vectors \mathbf{N}_c :

$$\mathbf{T} = \mathbf{R}\mathbf{N}_c^T(\mathbf{N}_c\mathbf{N}_c^T)^{-1} \quad (2)$$

The PQR bases \mathbf{V} are derived from principal component analysis (PCA) on a set of the metameric blacks specific to the device. The metameric blacks are spectral differences between the original spectra \mathbf{R} and the fundamental stimuli derived from the tristimulus values, expressed as:

$$\mathbf{B} = \mathbf{R} - \mathbf{T}\mathbf{N}_c \quad (3)$$

To make LabPQR into an ICS, only a limited number of eigenvectors should be preserved to reduce dimensions. Often the first three eigenvectors are preserved as the PQR bases:

$$\mathbf{V}_{PQR} = (\mathbf{v}_1, \mathbf{v}_2, \mathbf{v}_3) \quad (4)$$

where \mathbf{v}_i are eigenvectors approximating the metameric black correction to $\mathbf{T}\mathbf{N}_c$.

To explore the influence of dimensional reduction in LabPQR, the spectral representation portion in Eq. (4) will be changed by reducing the numbers of dimensions to two (PQ bases) and one (only a single P basis), respectively expressed as:

$$\mathbf{V}_{PQ} = (\mathbf{v}_1, \mathbf{v}_2) \quad (5)$$

and

$$\mathbf{V}_P = \mathbf{v}_1 \quad (6)$$

For Eq. (5), only the first two eigenvectors are preserved making for a five-dimensional LabPQR (or LabPQ) and for Eq. (6), only the most significant eigenvector is preserved making for a four-dimensional LabPQR (or LabP).

Spectral Gamut Mapping

Spectral gamut mapping can be considered from two viewpoints: colorimetric and spectral [5]-[6]. In one previous implementation [9], [12], the two gamut mappings were combined and considered simultaneously. Fractional area coverages of an inkjet printer for arbitrary requested spectra were computed by minimizing a single objective function: the weighted sum of CIEDE2000 color difference and the normalized Euclidian distance in PQR:

$$\text{ObjFunc1} = \text{Minimize}(\text{CIEDE2000} + k\Delta PQR) \quad (7)$$

where k is a weighting that may be empirically fitted.

The first term on the right hand side of Eq. (7) implies the absolute colorimetric matching based on the CIEDE2000 color difference while the second term represents spectral matching to minimize the spectral error between requested and response stimuli. Equation (7) can be globally utilized regardless of whether the requested stimuli are within the colorimetric or spectral response gamuts and is equivalent to minimizing spectral RMS error if the requested stimuli are within the colorimetric response gamut, because the Euclidian distance in PQR between a metameric pair is proportional to spectral RMS error [12]. For a particular response gamut, it was found that k of 50 performed well [12].

Interim Connection Space-Based Lookup Table

A six-dimensional LUT based on LabPQR is illustrated in Fig. 1. For purposes of illustration, the LUT is divided into two portions: CIELAB and PQR. Each node in the CIELAB portion is considered to hold a PQR sub-LUT containing sets of fractional area coverages at the nodes for when there are several different combinations of the fractional area coverages that yield distinct metamers under a given illuminant. When the LUTs based on five- and four-dimensional color spaces, LabPQ and LabP, were examined, the R and QR dimensions of the PQR sub-LUT were eliminated, respectively.

Equation (8) expressed the formula for calculating the size of a non-uniform LUT [4].

$$\text{SIZE}_{\text{bytes}} = \prod_{n=1}^{B_i} L_{i,n} \times B_o \times b_o \quad (8)$$

where b_o is the number of bytes per output band; B_o is the number of bands out; $L_{i,n}$ is the number of samples in the n th dimension; B_i is the number of bands in; and $\text{SIZE}_{\text{bytes}}$ is the size of the LUT in bytes.

For instance, the size of the six-dimensional $9 \times 9 \times 9 \times 9 \times 5 \times 5$ LabPQR is approximately 961KB where a six-color inkjet printer is used ($B_o = 6$) and all output bands are one byte each ($b_o = 1$). Clearly larger numbers of dimensions and nodes can provide higher reproduction accuracies, but the LUT size will become accordingly large. The size reduction of the ICS-based LUTs with respect to both dimensionality and the number of nodes is a critical issue for practical spectral color management.

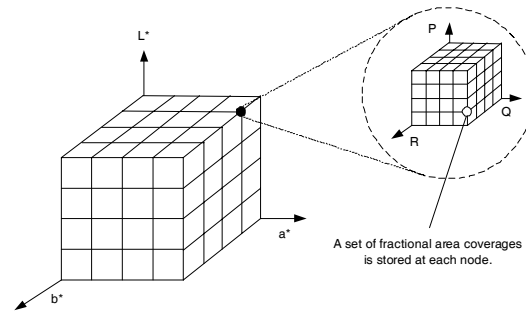


Figure 1. Six-dimensional LUT based on LabPQR.

Experimental

A Canon i9900 dye-based inkjet printer with a customized control driver was spectrally characterized for printer simulation. This printer had the capability of an eight-ink set, but only six were utilized: cyan (C), magenta (M), yellow (Y), black (K), red (R), and green (G). Spatial addressability of the inkjet printer was 1200 by 2400 dpi. All samples were printed on Canon Photo Paper Pro (PR-101) photo quality inkjet glossy paper. Spectral reflectance factor in the range between 400 and 700 nm was measured and colorimetric values were calculated under illuminant D50 and for the CIE 1931 2° standard observer.

A printer model similar to Chen, Berns, and Taplin's approach [13] was used to describe the CMYKRG inkjet printer's spectral characterization. This is based on the cellular Yule-Nielsen spectral Neugebauer model [14].

Workflow of Spectral Reproduction Evaluations

Using several different sizes of ICS-based LUTs, spectral reproductions with the use of the spectral printer model were evaluated. The workflows comprised of starting with a spectral image. The image was then transformed from spectra to LabPQR, further processed through the LUTs to find an appropriate set of fractional area coverages for the printer, a simulated printing was applied, and then the results were evaluated. To investigate the trade-off between the sizes of ICS-based LUTs and the reproduction accuracies, the reproduction accuracies at the different numbers of dimensions were evaluated.

In Fig. 2, the steps for evaluating the reproduction accuracies based on the spectral printer model are illustrated. First, LabPQR values were computed from spectra using the LabPQR transform that had been trained from 729 patches printed from the CMYKRg inkjet printer, which were randomly distributed in the CIELAB color space. Then, fractional area coverage values were chosen for each LabPQR, through a multi-dimensional linear interpolation technique in the ICS-based LUT. Spectral reflectances from a print were predicted using the spectral printer model, and spectral and colorimetric differences between the input and the predicted spectral reflectance factors were evaluated. In the evaluation of dimensionality, five-dimensional and four-dimensional LabPQRs were utilized as ICS in the spectral color management. For convenience, the five dimensional space will be referred to as LabPQ and the four dimensional space will be referred to as LabP. All the reproduction evaluations illustrated in Fig. 2 were completely computational.

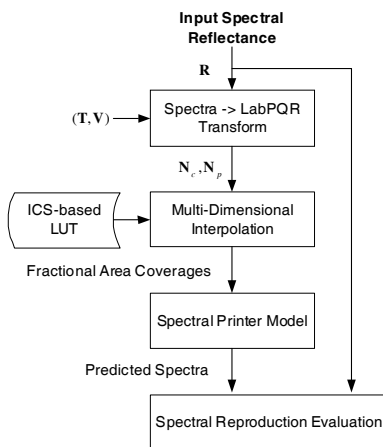


Figure 2. Schematic diagram for evaluating spectral reproduction accuracies based on the spectral printer model.

Grid Settings of Interim Connection Space-Based Lookup Tables

For the evaluations illustrated in Fig. 2, several different sizes of the ICS-based LUTs were populated. The numbers of grids in the CIELAB and PQR portions and the number of the PQR dimensions are summarized in Table I. Three different numbers of grids in the CIELAB portion, three different PQR dimensions (LabP, LabPQ, and LabPQR), and three different numbers of grids (increments) in the PQR portion were tested, in addition to a traditional CIELAB color space. Each grid was uniformly spaced

in LabPQR color space. Since the P basis is the most significant eigenvector approximating the metameric black set, as previously expressed in Eq. (4), the distribution range of the P values is the widest. Based on our previous research [12], the PQR values of typical object reflectance including the GretagMacbeth Color Checker and Color Checker DC are within (-1.2, 1.2), (-0.6, 0.6), and (-0.6, 0.6), respectively. The ranges of the ICS-based LUTs cover the typical PQR values.

Table I: Grid settings of the ICS-based LUTs.

CIELAB	P	PQ	PQR	PQR increment
33 x 33 x 33	13	13 x 7	13 x 7 x 7	0.2
17 x 17 x 17	9	9 x 5	9 x 5 x 5	0.3
9 x 9 x 9	5	5 x 3	5 x 3 x 3	0.6

Results and Discussion

Sizes of Interim Connection Space-Based Lookup Tables

Using Eq. (8), the sizes of the ICS-based LUTs at all the possible combinations of the dimensions and grid settings from Table I were calculated and are plotted in Fig. 3. For this calculation, all output bands were set to one byte each ($b_o = 1$). Note that the vertical axis is expressed in a logarithmic scale. The largest size of the six-dimensional 33x33x33x13x7x7 LabPQR LUT with PQR increment of 0.2 exceeded 130MB. In the authors' experience, LUTs more than 20MB may be unacceptable. Recall that the size of typical three-dimensional colorimetric LUT with 33x33x33 grids is about 100 times smaller at 211KB. In this research, LUTs exceeding 20MB were excluded. This affected the two largest LUTs (33x33x33x13x7x7 and 33x33x33x9x5x5).

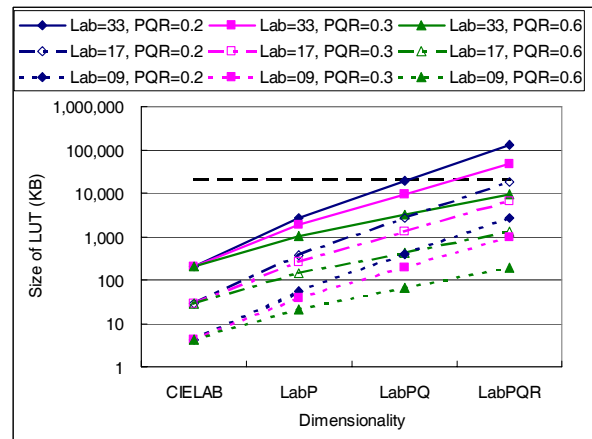


Figure 3. Sizes of the ICS-based LUTs at all the possible combinations of the dimensions and grid settings. Horizontal dashed line indicates 20MB.

Visualization of Interim Connection Space-Based Lookup Table

The fractional area coverages of the cyan ink in PQR at $(L^*, a^*, b^*) = (50, 0, 0)$ are plotted in Fig. 4 where darker circles indicates less use of the ink. The size of PQR portion of ICS-based LUT was 13x7x7. Each node yielded the exact same CIELAB value. The fractional area coverages changed smoothly

as the PQR values changed. As expected, the change of the fractional area coverages along the P axis was the largest while those along the R axis was the smallest. In other words, larger change of fractional area coverages tends to occur along the more significant axis in the spectral coordinates. For other color inks, a similar trend was seen in the PQ coordinates, and the fractional area coverages along the R axis seemed to be redundant. Thus, one may eliminate the least significant axis, R, from this ICS-based LUT and create five-dimensional LUTs. Similarly, the fractional area coverages of the cyan ink in a^*b^* coordinate at $(L^*, P, Q, R) = (50, 0, 0, 0)$ are plotted in Fig. 5. There was no serious discontinuity of the fractional area coverages in the LUT.

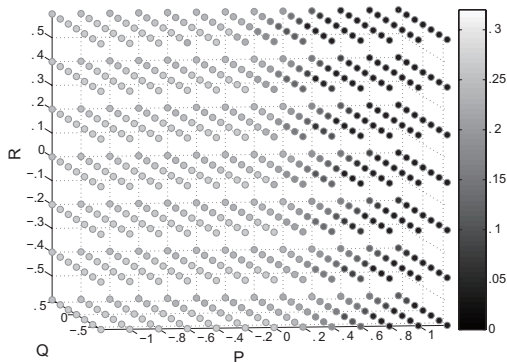


Figure 4. Fractional area coverages of the cyan ink in PQR of ICS-based LUT. Each node is located at the identical node in CIELAB, $(L^*, a^*, b^*) = (50, 0, 0)$.

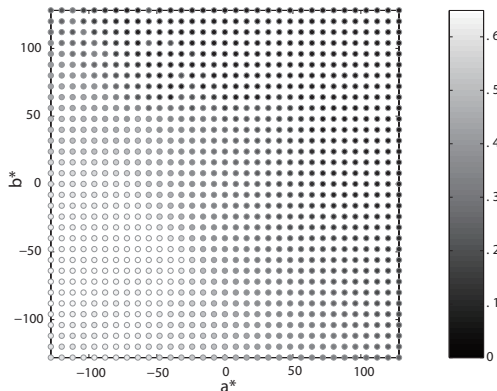


Figure 5. Fractional area coverages of the cyan ink in the a^*b^* coordinate at $(L^*, P, Q, R) = (50, 0, 0, 0)$.

Spectral Reproduction Accuracies based on the Spectral Printer Model

Using the Color Checker, the spectral reproduction accuracies based on the spectral printer model are summarized in Figs. 6 – 9, in comparison with the spectral reproduction accuracies where each output digit was directly calculated to minimize the objective function [Eq. (7)]. This comparative reproduction approach, expressed as “SGMA” (spectral gamut mapping algorithm), utilized no LUT and included no interpolation error of the LUT, so the SGMA did show the best spectral reproduction accuracies.

Three different numbers of the dimensions were examined, in addition to the traditional three-dimensional colorimetric-only approach.

Figures 6 and 7 illustrate average CIEDE2000 and spectral RMS errors for each size of the ICS-based LUT, respectively. As expected, a series of the $33 \times 33 \times 33$ LUTs in CIELAB indicated superior performance in terms of colorimetric accuracies. However, the colorimetric performances between the series of the $17 \times 17 \times 17$ and $33 \times 33 \times 33$ LUTs were not significantly large. Both series of the LUTs achieved sufficient colorimetric performance: average CIEDE2000 of less than unity. Since this evaluation did not include the printer variability, the colorimetric error between each LUT approach and the SGMA could only be caused by quantization introduced by the LUT. There was no correlation between the color difference, and the dimensionality of PQR. Mostly, the colorimetric reproduction accuracies depended on the LUT size in the CIELAB portion. The CIELAB LUT size did not influence the spectral reproduction accuracies, as shown in Fig. 7. The ICS-based LUTs indicated similar results depending on their number of dimensions. Note that there was no large spectral difference between each LUT approach and the SGMA, whereas there was large colorimetric difference between them. These results reveal that the linear interpolation in the PQR coordinates was successful in obtaining appropriate device output for spectral matching.

The predicted spectra were parametrically corrected [15] such that a perfect match was obtained under illuminant D50. A CIEDE2000 color difference was calculated for illuminant A and used as a metameric index (MI) [8], shown in Fig. 8. At five- and six-dimensional color spaces, LabPQ and LabPQR, all the average MIs were less than unity. (We consider that MI values less than unity indicate acceptable illuminant metamerism.) These results showed strong agreement with the previous research [9] that did not use a LUT. The five-dimensional LabPQ was sufficient to perform both colorimetric and spectral matching successfully. Smaller increments of PQR showed slightly superior performances.

The MI values of $9 \times 9 \times 9$ LUT series in CIELAB were smaller than their CIEDE2000s under illuminant D50 because parametric decomposition was performed before the calculation of color difference. These MI values do not represent actual color difference under illuminant A. To consider the color appearance of the predicted spectra under illuminant A, a CIEDE2000 color difference between the measured and the predicted spectra without the parametric decomposition was calculated for illuminant A, plotted in Fig. 9. Relatively large color differences were introduced for the $9 \times 9 \times 9$ LUT series, while the $17 \times 17 \times 17$ and $33 \times 33 \times 33$ LUT series at five-dimensional LabPQ still maintained sufficient performances, indicating average CIEDE2000s of less than unity.

Finally, statistics for the $17 \times 17 \times 17$ and $33 \times 33 \times 33$ LUT series at five-dimensional LabPQ are summarized in Table II, along with memory size of each LUT. It can be seen that there was no significant difference between all the LUTs with respect to the spectral RMS error. In terms of color difference, the $33 \times 33 \times 33$ LUTs were slightly superior to the $17 \times 17 \times 17$ LUTs, as discussed above. However, considering the memory size of the LUT, a series of the $17 \times 17 \times 17$ LUTs is remarkably smaller. Thus, the five-dimensional $17 \times 17 \times 17 \times 5 \times 3$ LUT with the PQ increment of

0.6, which requires 432KB, was deemed most successful in this evaluation.

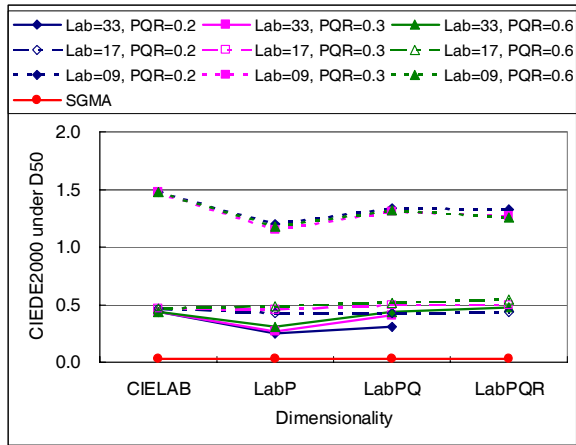


Figure 6. Average CIEDE2000 for each LUT size for the Color Checker at different numbers of dimensions.

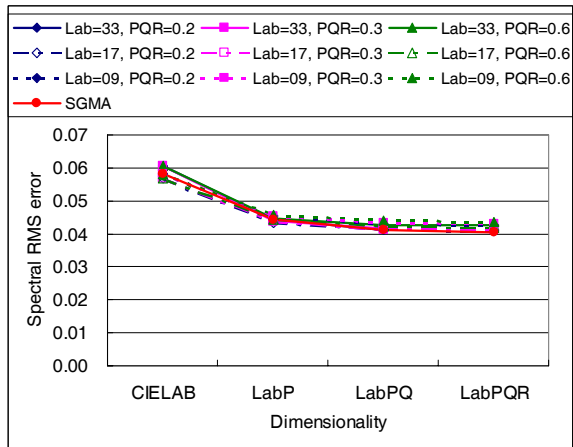


Figure 7. Average spectral RMS error for each LUT size for the Color Checker at different numbers of dimensions.

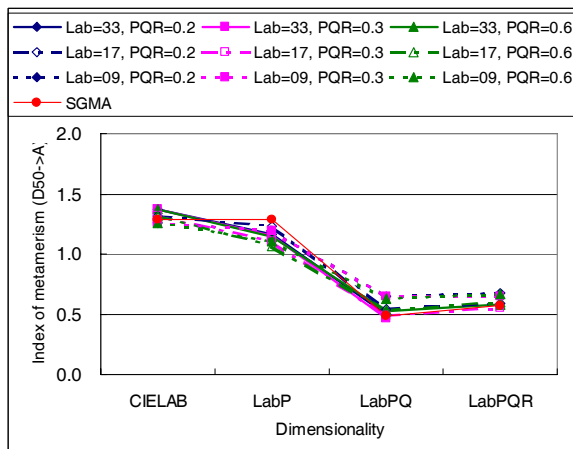


Figure 8. Average metameric index (MI) from illuminant D50 to illuminant A for each LUT size for the Color Checker at different numbers of dimensions.

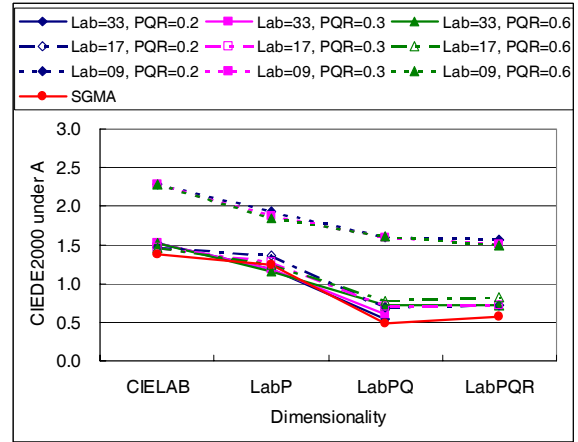


Figure 9. Average CIEDE2000 under illuminant A of each LUT size for the Color Checker at different numbers of dimensions.

Table II: Reproduction accuracies of the Color Checker using the 17x17x17 and 33x33x33 LUT series at five-dimensional LabPQ.

LUT type	CIEDE2000 (D50)			Spectral RMS error (%)		
	Ave.	Max.	Std. Dev.	Ave.	Max.	Std. Dev.
A	0.43	1.45	0.38	4.11	6.89	1.24
B	0.50	1.42	0.38	4.13	6.94	1.26
C	0.51	1.38	0.36	4.22	6.97	1.27
D	0.31	0.90	0.23	4.12	6.85	1.24
E	0.41	1.09	0.31	4.16	6.89	1.26
F	0.44	1.01	0.30	4.26	6.94	1.27
	MI (D50->A)			CIEDE2000 (A)		
LUT type	Ave.	Max.	Std. Dev.	Ave.	Max.	Std. Dev.
A	0.54	1.20	0.27	0.69	2.14	0.46
B	0.49	1.21	0.29	0.70	2.16	0.45
C	0.53	1.17	0.32	0.78	2.15	0.41
D	0.50	1.17	0.28	0.54	1.15	0.33
E	0.47	1.17	0.29	0.60	1.25	0.36
F	0.52	1.15	0.31	0.71	1.40	0.32

LUT type	CIELAB	PQ	PQR Increment	Size (KB)
A	17 x 17 x 17	13 x 7	0.2	2,620
B	17 x 17 x 17	9 x 5	0.3	1,295
C	17 x 17 x 17	5 x 3	0.6	432
D	33 x 33 x 33	13 x 7	0.2	19,162
E	33 x 33 x 33	9 x 5	0.3	9,476
F	33 x 33 x 33	5 x 3	0.6	3,159

Non-Uniform PQR Node Sampling

Since PQR axes are eigenvectors of metameric black corrections, PQR values tend to be centered about the origin of PQR coordinates. Non-uniform node sampling of ICS-based LUT that have relatively smaller increments of PQR values around the

origin may be an effective approach for reducing the size of the LUTs.

Table III summarizes the grid settings of non-uniform node sampling in the PQ axes in this evaluation. Because there was no significant difference of the reproduction from the five- to six-dimensional approaches, as previously discussed, only five-dimensional LUTs were tested. Reproduction accuracies for the Color Checker are summarized in Table IV. Compared with the results based on the uniform PQR node sampling, shown in Table II, the non-uniform PQR node sampling is effective for the LUT size reduction. For instance, the 17x17x17 CIELAB LUT with the non-uniform PQR node sampling indicates similar resultant data to the 17x17x17 CIELAB LUT with the regular PQR increments of 0.2, even though the former non-uniform sampling LUT required approximately half size of the latter uniform sampling LUT; the former LUT required 1,295KB and the latter LUT required 2,620KB. Similar results were obtained for the 33x33x33 LUT series in the CIELAB portion.

Table III: Grid settings of non-uniform node sampling in PQ.

	Nodes	# of nodes
P	-1.2, -0.8, -0.4, -0.2, 0, 0.2, 0.4, 0.8, 1.2	9
Q	-0.6, -0.2, 0, 0.2, 0.6	5

Table IV: Reproduction accuracies for the Color Checker using five-dimensional ICS-based LUTs with non-uniform node sampling in the PQ axes.

LUT type	CIEDE2000 (D50)			Spectral RMS error (%)		
	Ave.	Max.	Std. Dev.	Ave.	Max.	Std. Dev.
G	0.43	1.45	0.38	4.11	6.92	1.25
H	0.30	0.91	0.23	4.12	6.87	1.24
LUT type	MI (D50->A)			CIEDE2000 (A)		
	Ave.	Max.	Std. Dev.	Ave.	Max.	Std. Dev.
G	0.51	1.22	0.29	0.67	2.14	0.45
H	0.49	1.18	0.28	0.55	1.22	0.34

LUT type	CIELAB	PQ	PQR Increment	Size (KB)
G	17 x 17 x 17	9 x 5	Non-uniform	1,295
H	33 x 33 x 33	9 x 5	Non-uniform	9,476

Conclusions

Spectral color reproduction using an Interim Connection Space (ICS)-based lookup table (LUT) has been demonstrated. The ICS-based LUT was incorporated within spectral color management in LabPQR. Variations of the ICS-based LUT were evaluated with respect to quality trade-offs between size of the LUT and spectral reproduction accuracies, as well as the number of dimensions necessary for spectral color management. Our experiments based on a spectral printer model have revealed that the five-dimensional 17x17x17x5x3 LUT with PQ increment of 0.6 (17x17x17 in CIELAB and 5x3 in PQ), which requires 432KB, was optimal. For the GretagMacbeth Color Checker, this five-dimensional LUT resulted in sufficient reproduction accuracies:

average CIEDE2000 of 0.51 and average spectral RMS error of 4.22 %.

A future direction of this research will be to print images and to test actual reproduction accuracies using a lookup-table (LUT) based on LabPQR. A new metric that can evaluate spatial spectral reproduction accuracies will be desirable. Another consideration is to test different printers. The number of dimensions in the ICS is highly printer dependent. Testing the reproduction of printers with different number and types of inks would be obviously of interest.

References

- [1] M.R. Rosen, F.H. Imai, X. Jiang and N. Ohta, "Spectral Reproduction from Scene to Hardcopy II: Image Processing", Proc. SPIE, **4300**, pp.33-41 (2001).
- [2] M.R. Rosen, L.A. Taplin, F.H. Imai, R.S. Berns, and N. Ohta, "Answering Hunt's Web Shopping Challenge: Spectral Color Management for a Virtual Swatch", Proc. Ninth CIC, pp.267-273 (2001).
- [3] M.R. Rosen, "Navigating the Roadblocks to Spectral Color Reproduction: Data-Efficient Multi-Channel Imaging and Spectral Color Management", Ph.D. Dissertation, Rochester Institute of Technology, Rochester, New York (2003).
- [4] M.R. Rosen and N. Ohta, "Spectral Color Processing Using an Interim Connection Space", Proc. 11th CIC, pp. 187-192 (2003).
- [5] M.W. Derhak and M.R. Rosen, "Spectral Colorimetry using LabPQR - An Interim Connection Space", J. Imaging Sci. and Technol., **50**, pp.53-63 (2006).
- [6] M.R. Rosen and M.W. Derhak, "Spectral Gamuts and Spectral Gamut Mapping", Proc. SPIE, **6062**, (2006).
- [7] G. Wyszecki and W. Stiles, Color Science, 2nd Edition, John Wiley & Sons (1982).
- [8] R.S. Berns, Billmeyer and Saltzman's Principles of Color Technology, 3rd Edition, John Wiley & Sons (2000).
- [9] S. Tsutsumi, M.R. Rosen and R.S. Berns, "Spectral Color Management using Interim Connection Spaces based on Spectral Decomposition", Proc. 14th CIC, pp. 246-251 (2006).
- [10] P. Hung, "Colorimetric Calibration in Electronic Imaging Devices using a Look-Up-Table Model and Interpolations", J. Electron. Imaging, **2**, pp. 53-61 (1993).
- [11] R. Balasubramanian, "Reducing the Cost of Lookup Table based Color Transformations", J. Imaging Sci. and Technol., **44**, pp. 321-327 (2000).
- [12] S. Tsutsumi, M.R. Rosen and R.S. Berns, "Spectral Gamut Mapping using LabPQR", J. Imaging Sci. and Technol., *in press* (2007).
- [13] Y. Chen, R.S. Berns and L.A. Taplin, "Six Color Printer Characterization Using an Optimized Cellular Yule-Nielsen Spectral Neugebauer Model", J. Imaging Sci. and Technol., **48**, pp.519-528 (2004).
- [14] D.R. Wyble and R.S. Berns, "A Critical Review of Spectral Models Applied to Binary Color Printing", Color Res. Appl. **25**, 5-19 (2000).
- [15] H.S. Fairman, "Metameric Correction Using Parametric Decomposition", Color Res. Appl. **12**, pp.261-265 (1987).

Author Biography

Shohei Tsutsumi received his B.E. and M.E. degrees in Electrical Engineering from Keio University, Japan in 1996 and 1998, respectively. He joined Canon Inc. in 1998 to work on development of novel approaches to image processing including halftoning and image quality. He has developed some pictorial inkjet printers such as PIXMA iP 8500 and i9900. From 2004 to 2006, he was a visiting scientist at the Munsell Color Science Laboratory, Rochester Institute of Technology. He is a member of Society for Imaging Science and Technology.